Tribology International 185 (2023) 108563

Contents lists available at ScienceDirect

Tribology International

journal homepage: www.elsevier.com/locate/triboint

Frictional half plane contacts subject to varying normal load and bulk tension under various load paths with application to fretting fatigue experiments

J.P.J. Truelove *, L.E. Blades, D.A. Hills, R.J.H. Paynter

Department of Engineering Science, University of Oxford, Parks Road, Oxford, OX1 3PJ, UK

ARTICLE INFO

Keywords:
Contact mechanics
Fretting
Fatigue

ABSTRACT

In many fretting fatigue experiments the loads applied to the contact are sinusoidal and in phase, creating a straight line path through load space. Although this form of loading is a good representation of many of the load histories present in engineering assemblies, the usefulness of this form of load cycle when investigating the causes of fretting fatigue damage is limited. In this paper we first review solutions for uncoupled half plane contacts under bulk tension and normal loading, then develop some novel load paths with properties that are desirable in fretting fatigue experiments. Throughout this paper the results are illustrated via application to a Hertzian contact, although the principles apply to any contact capable of representation using half-plane theory.

1. Introduction

The understanding of frictional contacts subject to varying normal loads and bulk tension is of great importance in predicting the failure of components under fretting fatigue. Examples arise in all manner of engineering assemblies, such as those found at the roots of fan blades in a gas turbine engine, or those used in wellhead connectors.

In many of these applications the contact will experience a complex, multi stage load cycle. In a fan blade the contact experiences a combination of centrifugal and vibrational loading, in a well head connector a contact will experience forces arising from both the clamping action of the connector and, indirectly, the action of waves.

Many experimental investigations into fretting fatigue involve exposing a contact to cyclic, usually sinusoidal, variations in loads around a fixed midpoint. While such experiments are straightforward to design and relatively simple to analyse, this greatly limits the range of behaviour that it is possible to investigate, most experiments being confined to looking at straight line load 'cycles' between two points in load space.

In this paper we will first present various known solutions for contacts following a range of paths in a normal load-bulk tension load space. The contacting bodies are elastically similar, and one is subject to a bulk tension, σ. These solutions are used to construct load histories with certain desirable properties: for example, we can create load paths which start and end at the same points in load space but where one gives rise to slip and one is under conditions of full stick, or we can create load paths where slip occurs in only one direction, or we can create load path loops that have equal but opposite shear traction and slip behaviour when the order of loading is reversed.

Throughout this paper we will adopt the notation devised by Barber et al. [1] where possible, the contact half width is written in the form $a_i(P_i)$, where P_i is the applied normal load, and the corresponding contact pressure distribution is given by $p_i(x, P_i)$, $x \in a_i$.

2. Full stick

First, we consider the problem of a contact which remains fully stuck throughout the loading path, so that no slip occurs. The two factors that determine whether a contact will remain stuck are the load path taken and the coefficient of friction.

2.1. Constant normal load

When a bulk tension is applied to a contact under constant normal loading, so that the location of the edge of contact does not move, the resulting change in shear traction, $\Delta q(x; P)$, is singular and is given by [2]

$$\Delta q(x; P) = \frac{x\Delta\sigma}{4\sqrt{a(P)^2 - x^2}}. \tag{1}$$

It is worth noting that this result is independent of the form of the contact or the contact pressure distribution, it depends only on the contact width. Since the shear traction is singular at the edge of contact this implies that an infinite coefficient of friction is required to prevent slip.

* Corresponding author.
E-mail address: james.truelove@eng.ox.ac.uk (J.P.J. Truelove).

https://doi.org/10.1016/j.triboint.2023.108563
Received 21 December 2022; Received in revised form 21 April 2023; Accepted 2 May 2023
Available online 5 May 2023

2.2. Varying normal load

We now consider what happens when there is a simultaneous change in normal load, dP, and tension $d\sigma$. For an infinitesimal increment in contact force, the increment of contact pressure is given by [2]

$$dp(x;P) = \frac{dP}{\pi\sqrt{a(P)^2 - x^2}} \tag{2}$$

whereas for an infinitesimal increment in bulk tension, the increment of shear traction is [2]

$$dq(x;P) = \frac{x d\sigma}{4\sqrt{a(P)^2 - x^2}} \tag{3}$$

Because the shear traction has a multiplier, x, in its numerator the maximum ratio of shear traction to pressure will occur at the edges of contact, $x = \pm a$. To prevent slip the ratio of shear traction to contact pressure must be less than the coefficient of friction [2], so that the change in loads must satisfy the inequality

$$\frac{d\sigma}{dP} < \frac{4\mu}{\pi a(P)}, \tag{4}$$

where μ is the coefficient of friction. Often it is more convenient to express this limit in terms of the change in bulk tension with respect to the contact half width, so that, equivalently,

$$\frac{d\sigma}{da} < \frac{4\mu}{\pi a(P)}\frac{dP}{da}. \tag{5}$$

2.3. Behaviour when following an increasing normal load path

Above we gave the solution for the application of bulk tension under a fixed normal load, and showed how this form of loading would always result in slip, except in the unrealistic case of an infinite coefficient of friction. Let us now extend the analysis to look at loading cycles where both the normal load and bulk tension vary together, with finite friction. If the gradient of this load path satisfies inequality (4) the contact will remain fully stuck. This form of loading, with multiple load components varying together, occurs frequently in real contacts, for example in a gas turbine during acceleration the centripetal force on a blade generates a change in both the contact pressure and shear traction at the dovetail root due to the angled contact surface. Let us consider the behaviour of a contact loaded from a point (P_1, σ_1) to (P_2, σ_2) along a straight line in $P - \sigma$ space, so that

$$\frac{d\sigma}{dP} = \frac{\sigma_2 - \sigma_1}{P_2 - P_1}. \tag{6}$$

By integrating equation (2) we can write the change in contact pressure as

$$\Delta p(x)^{1\to 2} = \int_{P1}^{P2} \frac{dP}{\pi\sqrt{a^2 - x^2}} = p(x, P_2) - p(x, P_1), \tag{7}$$

and by integrating equation (3) we can write the change in shear traction as

$$\Delta q(x)^{1\to 2} = \int_{\sigma_1}^{\sigma_2} \frac{x}{4\sqrt{a^2 - x^2}} d\sigma. \tag{8}$$

Changing from an integral over σ to an integral over P through $d\sigma = \frac{d\sigma}{dP}dP$ and simplifying produces

$$\Delta q(x)^{1\to 2} = \int_{P_1}^{P_2} \frac{x}{4\sqrt{a^2 - x^2}}\frac{d\sigma}{dP}dP = \frac{\pi x}{4}\frac{\sigma_2 - \sigma_1}{P_2 - P_1}\int_{P_1}^{P_2} \frac{dP}{\pi\sqrt{a^2 - x^2}} \tag{9}$$

where the solution of the integral is just the change in contact pressure. The change in shear traction moving from point 1 to point 2 is therefore given by

$$\Delta q(x)^{1\to 2} = \frac{\pi x}{4}\frac{\sigma_2 - \sigma_1}{P_2 - P_1}\left[p\left(x;P_2\right) - p\left(x;P_1\right)\right], \tag{10}$$

which corresponds to the change in contact pressure multiplied by x, the gradient of loading and a constant factor of $\pi/4$. An example of the resultant shear traction for a fully stuck contact under varying load paths in $P - \sigma$ space is shown in Fig. 1, for both Hertzian and flat and rounded geometries, illustrating the load path dependence of the solution, and how the stress field becomes more nearly singular as the gradient of the second step of loading increases.

3. Partial slip

Having looked at the behaviour of a contact under conditions of full stick, let us now look at the solution when slip occurs. A contact where the tangentially loading arises just from bulk tension cannot experience *sliding* as the slip at each end of the contact is in opposite directions and an infinite bulk tension would be required for the slip zone to reach the centre of the contact.

3.1. Finding the size of the slip zone

The study of a Hertzian contact under a fixed normal load and increasing bulk tension was solved numerically by Nowell and Hills [3] and in closed form by Ciavarella and Macina [4]. These solutions were found by noting two properties of the contact — in the stick zone there is no relative displacement of the two surfaces, while in the slip zone the shear traction is the contact pressure multiplied by the coefficient of friction. Combining these two conditions defines an integral equation, the side condition of which provides the stick zone size, and the solution of which produces the shear traction. As an example, for a 2D Hertzian contact with radius R and contact half width a the size of the stick zone, a_K is given by [4]:

$$\frac{\sigma\pi R}{8a\mu E^*} = K\left(\sqrt{1 - \frac{a_K^2}{a^2}}\right) - E\left(\sqrt{1 - \frac{a_K^2}{a^2}}\right) \tag{11}$$

or, in terms of the applied normal load

$$\frac{\sigma}{16\mu}\sqrt{\frac{\pi^3 R}{PE^*}} = K\left(\sqrt{1 - \frac{P_K}{P}}\right) - E\left(\sqrt{1 - \frac{P_K}{P}}\right) \tag{12}$$

and the shear traction distribution is given by:

$$q(x) = sgn(x)\mu p(x;P) \quad a_K < |x| < a$$

$$q(x) = \frac{2\mu E^*}{\pi}\frac{x}{R}\sqrt{\frac{a_K^2 - x^2}{a^2}}\left[\Pi\left(\sqrt{\frac{a^2 - a_K^2}{a^2 - x^2}}, \sqrt{1 - \frac{a_K^2}{a^2}}\right) - K\left(\sqrt{1 - \frac{a_K^2}{a^2}}\right)\right] \quad |x| < a_K$$

where $K(k)$, $E(k)$ and $\Pi(n,k)$ are, respectively, complete elliptic integrals of the first, second and third kinds.

A plot of a typical shear traction distribution is given in Fig. 2, showing the zones of slip at each end of the contact.

4. Varying normal load with a two step loading regime

It is useful to consider what happens in a more general sense when a contact follows a load path constructed so that during the first part of the load path the contact is stuck, and during a subsequent load step slip occurs. By using a load path of this form a shear traction distribution can be locked into the contact before slip occurs. A simple example load path of this kind consists of two steps, as shown in Fig. 3; the contact is first taken from an unloaded state to a point (P_1, σ_1) under conditions of full stick, then further loaded to a point (P_2, σ_2), following a path such that slip occurs in the second stage of loading and where $P_2 > P_1$.

A loading step where the contact remains stuck locks a distribution of surface strains into the contact, which result in a shear traction

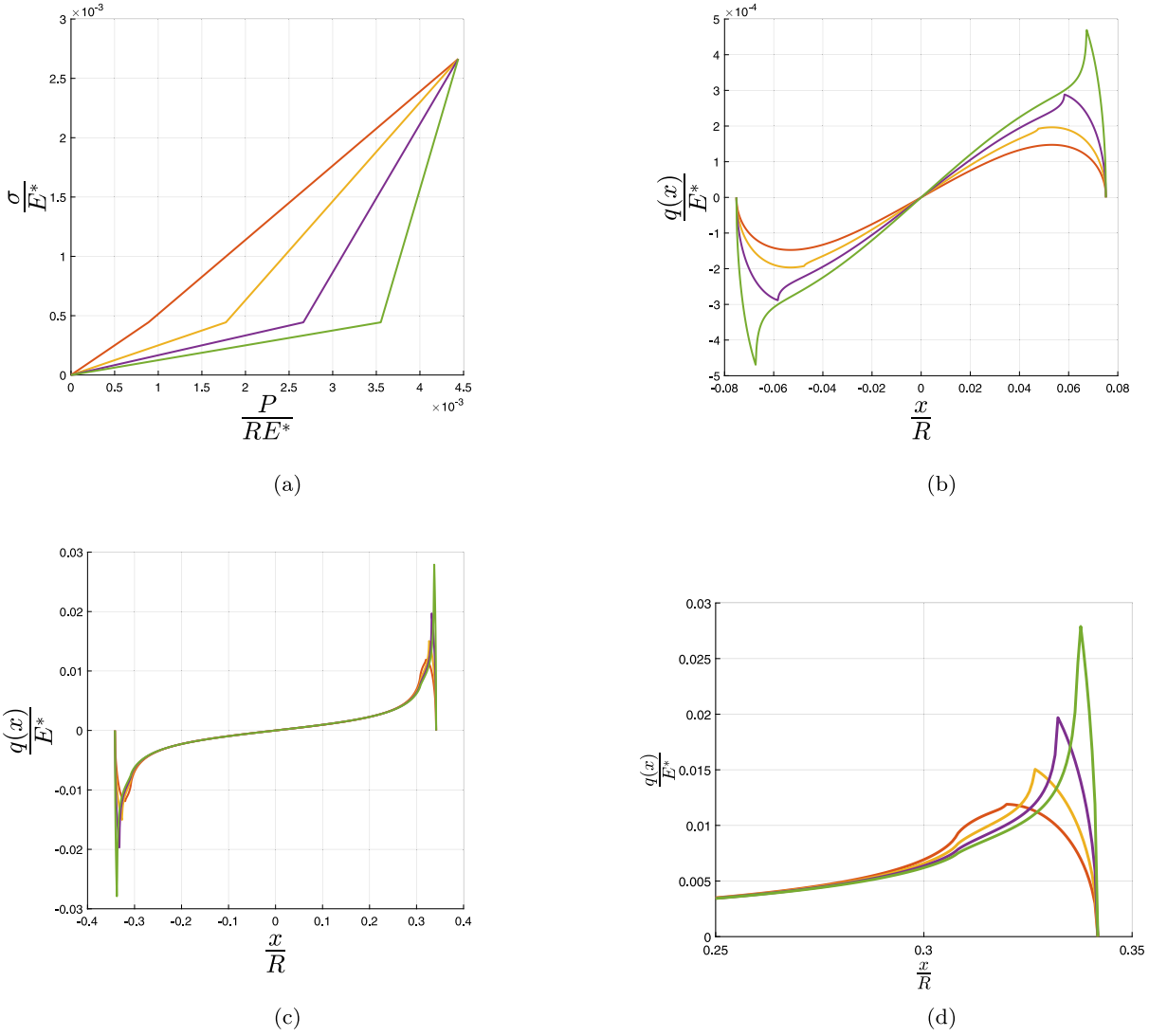

Fig. 1. The shear traction distributions for fully stuck Hertzian and flat and rounded contacts under varying load paths. The hertzian contact has radius R, the flat and rounded contact has half width a and corner radius R, with a/R equal to $4/13$. (a) The loading paths taken through $P-\sigma$ space, (b) The resultant shear traction distribution for a fully stuck Hertzian contact taken through the loading paths shown in Fig. 1(a), (c) The shear traction distributions for a fully stuck flat and rounded contact at the end point of the loading paths shown in Fig. 1(a), (d) A zoomed in view of Fig. 1(c), showing the shear traction at the edge of the contact.

distribution. If the contact then follows a load path so that it slips the solution during the slipping stage will have the properties that in the slip zones the shear traction is the contact pressure multiplied by the coefficient of friction, μ, while in the stick zone there is no relative tangential displacement between the two surfaces — the surface strains from the initial loading step are therefore preserved only in the region that does not slip. As shown in Ramesh et al. [5], the solution can therefore be found by superimposing a partial slip shear traction distribution onto a full stick solution, consisting of the original stuck shear traction preserved only in the stick zone. This is because loading a contact along a path from P_1 to P_2 so that the contact slips during the later part of loading, creating a slip zone of size $a_k(P_k)$, is equivalent to loading the contact from P_1 to P_k along a fully stuck load path, then loading the problem sequentially from P_k to P_2, first applying the normal load to grow the contact to its full extent, then applying the bulk tension to create a slip zone extending from $a(P_2)$ to $a(P_k)$. The size of the stick zone when there is a pre-existing shear traction can be found by looking for the intersection of Eq. (11) with a previously stuck point on the cycle, or another line defined by Eq. (11) from prior slip, this is illustrated for the two step loading shown in Fig. 3(a). The resulting shear traction for these load paths is shown in Fig. 3(b), where it can be seen clearly how changing the load path results in different shear traction distributions and slip zone sizes for the same final point in load space.

Since the condition for full stick is a function of the contact half width, $a(P)$, the maximum gradient of loading in (P,σ) space will change as the normal load increases. For incomplete contacts, such as a Hertzian, the contact width will grow larger as the normal load increases, so that the maximum gradient of loading will decrease.

Fig. 4 shows examples of two step load paths, and the constructions giving the boundaries for various types of behaviour as applied to a Hertzian contact. In this load cycle the contact starts at a point (P_1,σ_1) and is loaded at a constant bulk tension to an intermediate point (P^*,σ_1). The contact is then loaded along a straight line to the maximum load point (P_2,σ_2). Limiting cases of this load path are given by $P^*=P_1$, which represents a purely proportional loading between these two points, and $P^*=P_2$, which represents a sequential loading (shown in black). For intermediate values of P^* a range of different behaviours can occur.

Let us start at the minimum value of P^*, $P^*=P_1$ and consider what happens as the value of P^* increases. In this case the two load points have been chosen such that the proportional loading path is fully stuck

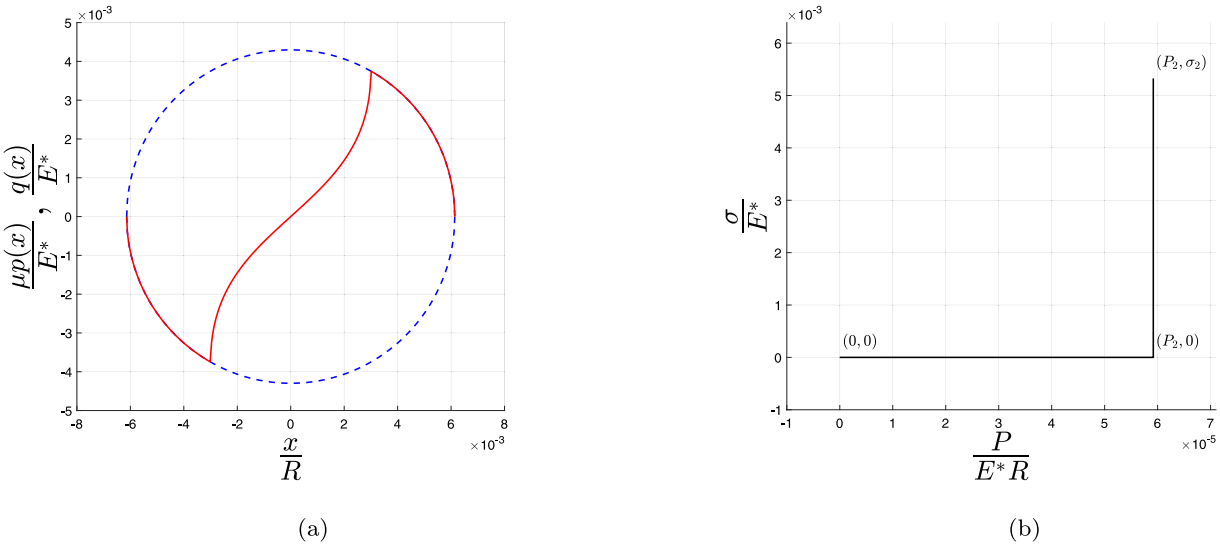

Fig. 2. The shear traction distribution (a) for a Hertzian contact experiencing partial slip following a sequential loading, as illustrated in (b). The blue dashed lines show the contact pressure envelope, multiplied by the coefficient of friction, while the red line shows the shear traction distribution. Several notable features are visible, including the anti-symmetric form of the shear traction distribution, the slip zones of equal size but opposite direction, and the zero crossing in the shear traction at the centre of the contact.

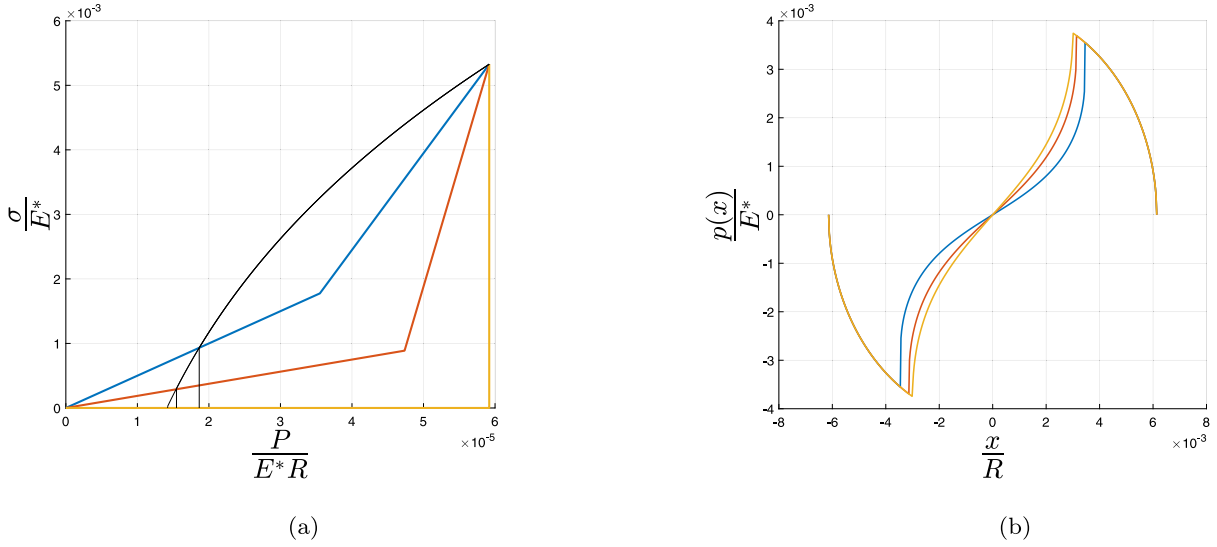

Fig. 3. The constructions used to find the size of the stick zone and resultant shear traction distributions for a hertzian contact following a two step load path. (a) The load paths and construction used to find the size of the stick zone in non-dimensional P, σ space, (b) The resultant shear traction distribution for a contact loaded following the path in Fig. 3(a).

throughout the loading process, and inequality (4) is not violated at any point during the proportional loading. Further, any load path where the value of P^* is smaller than the value of P where the red line intersects the constant bulk tension loading will be fully stuck throughout the entire loading cycle, as the red line has a gradient so that inequality (4) is not violated.

As the position of P^* moves to the right of the red line slip will occur, but for points to the right of the green line this will only in certain parts of the loading cycle, not throughout the entire second step of loading. Inequality (4) is a function of the contact half width, with lower gradients of loading required to initiate slip for larger contacts, so following a straight line load path in load space will result in slip occurring first at the maximum value of P.

For values of P^* which lie between the red and green lines of Fig. 4 slip will only occur at large values of P, i.e. as the second step of loading approaches (P_2, σ_2). The construction for finding the size of the stick zone at (P_2, σ_2) is given by Eq. (11), shown here in blue dots, and the load path where the value of $P^* = P_k$ is shown as a blue chain line. Using this the zone between the red and green lines can be subdivided further: load paths which lie between the red and blue lines will have final stick zone sizes defined by the intersection of the stick zone construction with the second stage of loading, so that the size of the stick zone depends upon P^*, whereas load paths lying between the blue and green lines will have stick zone sizes defined by the intersection of the stick zone construction with the line of constant σ loading, the size of the stick zone is the same for all load paths and is independent of P^*, though the slip displacements will differ.

Finally let us continue to increase the value of P^* so that the loading paths now lie to the right of the green line in Fig. 4. Once the value of P^* reaches this level the gradient of loading in the second step of the cycle is now sufficient to ensure that inequality (4) is violated at all points throughout the second stage of loading, and so slip initiates as soon as the second stage of loading begins. The final size of the stick zone is again given by the intersection of the construction line with the line of constant σ loading and as such is independent of the loading path, though the slip displacements will vary.

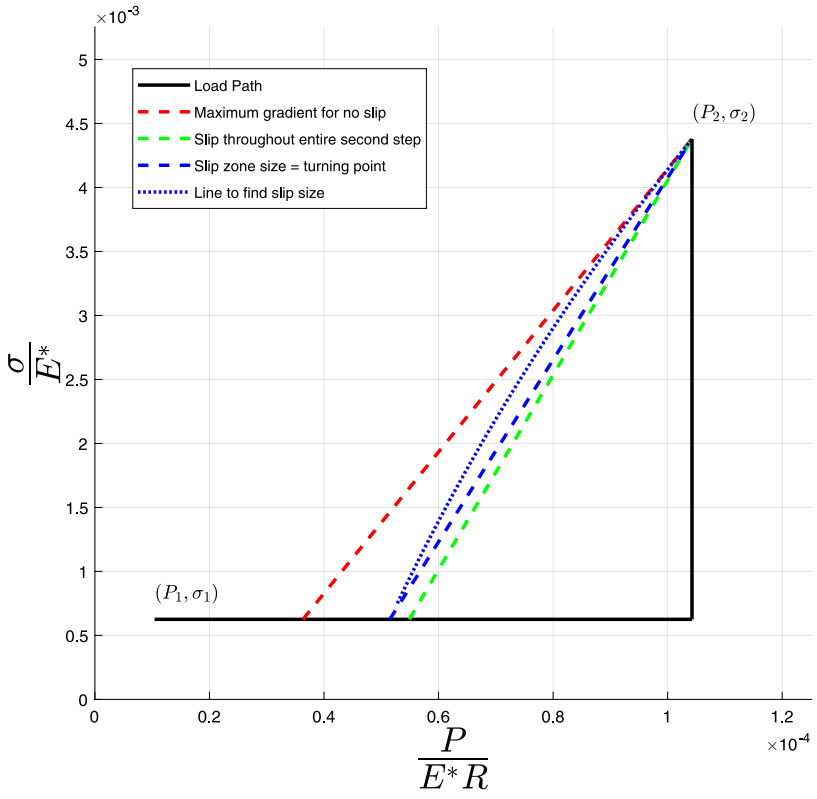

Fig. 4. A plot showing the various regimes of behaviour that can occur when a contact is loaded along a two step path in (P, σ) space.

5. Cyclic loading

In many real contacts the loading will be driven by some kind of varying or fluctuating process, so that the loading may vary cyclically in time. This kind of loading may occur, for example, in the hub of a turbofan engine where centripetal forces are developed during engine acceleration and deceleration, or, in our wellhead connector example, from the action of the waves. In these kinds of problems understanding the steady-state behaviour of the contact is of great importance, as damage may occur over tens of thousands or hundreds of thousands of loading cycles. As in the partial slip case the solutions found depend upon a knowledge of the contact law, so we will restrict ourselves to a Hertzian geometry for simplicity.

A load cycle that occurs frequently is one where the bulk tension and normal load both oscillate in phase. The results given here are a simplified form of the results found by Ramesh et al. [5], who considered the more general case of a loading cycle with an arbitrary phase shift.

For a contact loaded with a shear force the size of the stick zones can be found through direct application of horizontal equilibrium to the various components of the Cattaneo–Mindlin solution [1], this is equivalent graphically to looking for intersections of lines of gradient $\pm\mu$ with the loading paths though P, Q space.

For a contact under bulk tension loading the no slip condition is a function of a, so it is often more convenient to use the contact half width as a measure of normal load and instead move through a, σ space. For a Hertzian contact, for example, the maximum gradient of loading for no slip is then a constant, given by

$$\frac{d\sigma}{da} = \frac{2\mu E^*}{R} \tag{13}$$

The lines whose intersections define the size of the stick zone during loading and unloading are curves with form depends upon the geometry, for a Hertzian contact they are defined by [5]:

$$\bar{\sigma} = \bar{\sigma}_1 + \frac{4\mu\bar{a}_1}{\pi}\left[K\left(\sqrt{1-\left(\frac{\bar{a}}{\bar{a}_1}\right)^2}\right) - E\left(\sqrt{1-\left(\frac{\bar{a}}{\bar{a}_1}\right)^2}\right)\right] \tag{14}$$

during unloading and

$$\bar{\sigma} = \bar{\sigma}_2 - \frac{4\mu\bar{a}_2}{\pi}\left[K\left(\sqrt{1-\left(\frac{\bar{a}}{\bar{a}_2}\right)^2}\right) - E\left(\sqrt{1-\left(\frac{\bar{a}}{\bar{a}_2}\right)^2}\right)\right] \tag{15}$$

during loading, so that the size of the steady state stick zone during cyclic loading, $\bar{a_K}$ is given by

$$\begin{aligned}\left(\frac{\pi}{4}\right)\left(\frac{\bar{\sigma}_2 - \bar{\sigma}_1}{\mu}\right) = \bar{a}_1\left[K\left(\sqrt{1-\left(\frac{\bar{a}_K}{\bar{a}_1}\right)^2}\right) - E\left(\sqrt{1-\left(\frac{\bar{a}_K}{\bar{a}_1}\right)^2}\right)\right] \\ +\bar{a_2}\left[K\left(\sqrt{1-\left(\frac{\bar{a}_K}{\bar{a}_2}\right)^2}\right) - E\left(\sqrt{1-\left(\frac{\bar{a}_K}{\bar{a}_2}\right)^2}\right)\right].\end{aligned} \tag{16}$$

where $\bar{a}$ and $\bar{\sigma}$ are non-dimensional groups, defined by

$$\bar{\sigma} = \frac{\sigma}{E^*} \quad \bar{a} = \frac{a}{R}. \tag{17}$$

Let us now consider how we determine the state of stress at each point in the loading cycle, for the load path in black in Fig. 5. In this cycle a contact is first loaded proportionally from an unloaded point to a point (P_1, σ_1) without slip. The contact is then loaded further to a point (P_2, σ_2), where the gradient of loading is sufficient to ensure that slip occurs at *all* points along the second stage of loading. The contact is then cyclically loaded between (P_1, σ_1) and (P_2, σ_2) resulting in a zone of reversing slip.

In the upper graph of each sub figure the black lines show the load path, with the arrows showing the direction of loading in the current step and the red dot showing the current values of P and σ (denoted P^* and σ^* in the following discussion). The green solid lines show the construction for the transient problem, the red and blue solid lines show

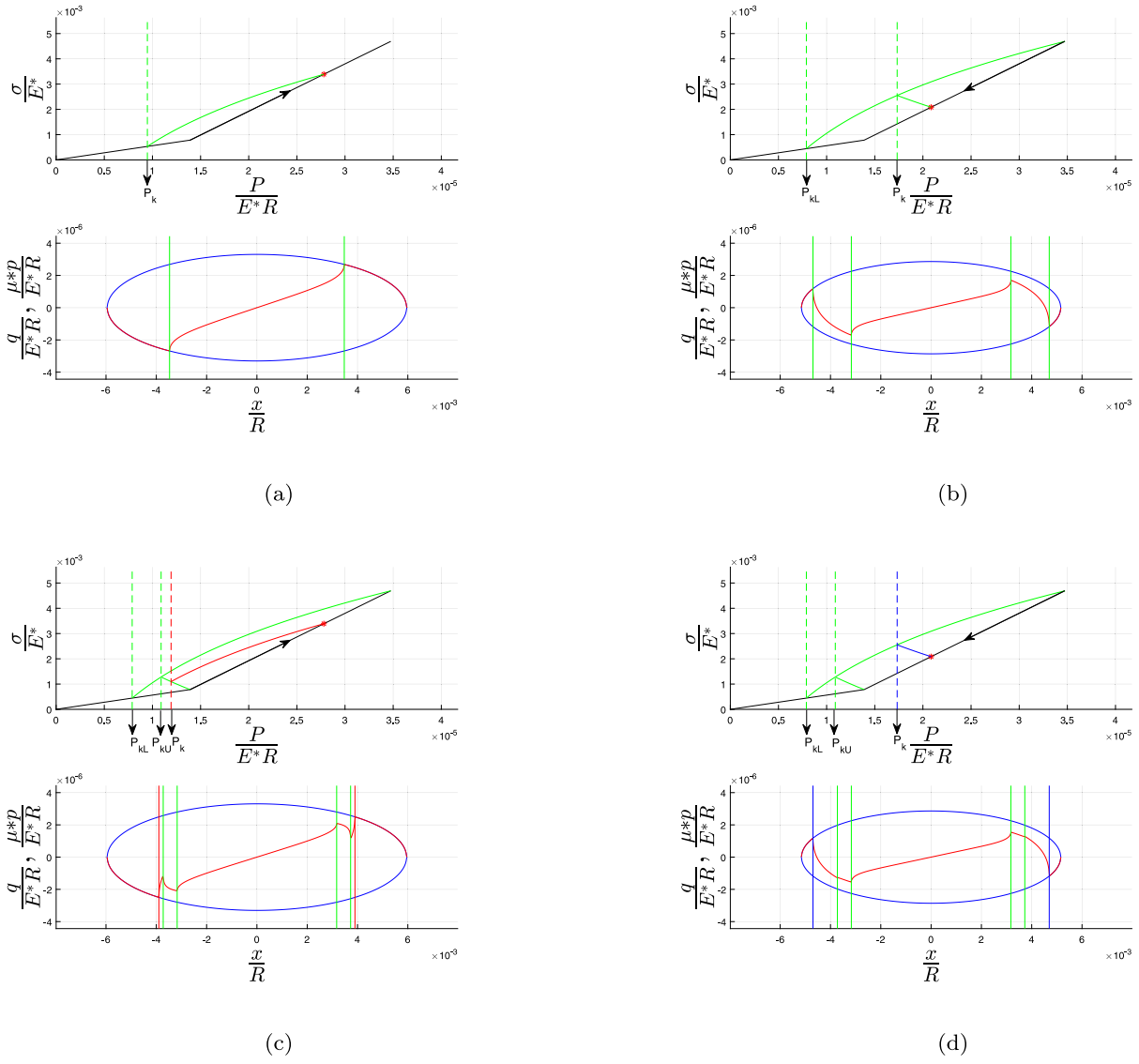

Fig. 5. Shear traction distributions and stick zone constructions for a Hertzian contact under a cyclic loading cycle. (a) The stick zone construction and shear traction distribution during the transient loading step of a cyclic loading cycle, (b) The stick zone construction and shear traction distribution during the transient unloading step of a cyclic loading cycle, (c) The stick zone construction and shear traction distribution during the steady state loading step of a cyclic loading cycle, (d) The stick zone construction and shear traction distribution during the steady state unloading step of a cyclic loading cycle.

the construction during the steady state. The vertical dashed lines show the points of intersection, and correspondingly the normal load used to calculate the size of the slip zone.

The lower graph of each sub figure shows the shear traction distribution at each point in the cycle. The shear traction is shown in red, the contact pressure multiplied the coefficient of friction in blue. The vertical lines show the location of the slip/stick transition point, with each line's location corresponding to the size of the contact at the loads in the upper figure.

In the first step of loading the contact is loaded from an unloaded state to (P_1, σ_1), with the contact remaining fully stuck. The solution for this stage of loading is the same as that discussed in Section 2, and the shear traction at normal load P^* is given by

$$q(x; P^*) = q_{FS}(x; P^*) \tag{18}$$

where

$$q_{FS}(x; P^*) = \frac{\sigma_1}{P_1}\frac{\pi x}{4} p(x; P^*). \tag{19}$$

In the second step of the cycle the contact is loaded from (P_1, σ_1) to (P_2, σ_2), with the gradient of loading being sufficient to ensure that slip occurs at all points during this phase. The stick zone construction and shear traction distribution are the same as those discussed in Section 4, and are shown in Fig. 5(a). The shear traction distribution at a load P^* is therefore given by

$$q(x; P^*) = q_{FS}(x; P_k) + q_{PS}(x; P^*; P_k) \tag{20}$$

where P_k is the load corresponding with the size of the stick zone, found from the intersection of a line defined by Eq. (15) with the first stage of the loading path, and $q_{PS}(x; P^*; P_k)$ is a partial slip shear traction distribution with overall size corresponding to load P^* and stick zone size corresponding to P_k. The size of the stick zone at the end of this loading step is henceforth denoted $a(P_{kL})$.

The third step of the cycle consists of the contact being unloaded from (P_2, σ_2) to (P_1, σ_1). As the gradient of unloading is greater than the frictional limit at all points during the unloading cycle reverse slip will occur. The shear traction therefore now has three components, a full stick term preserved only over the region that has never slipped, a reverse slip term which extends from the edge of contact to the unloading stick zone size, and a forward slip component between the other two distributions, representing the proportion of the slip from

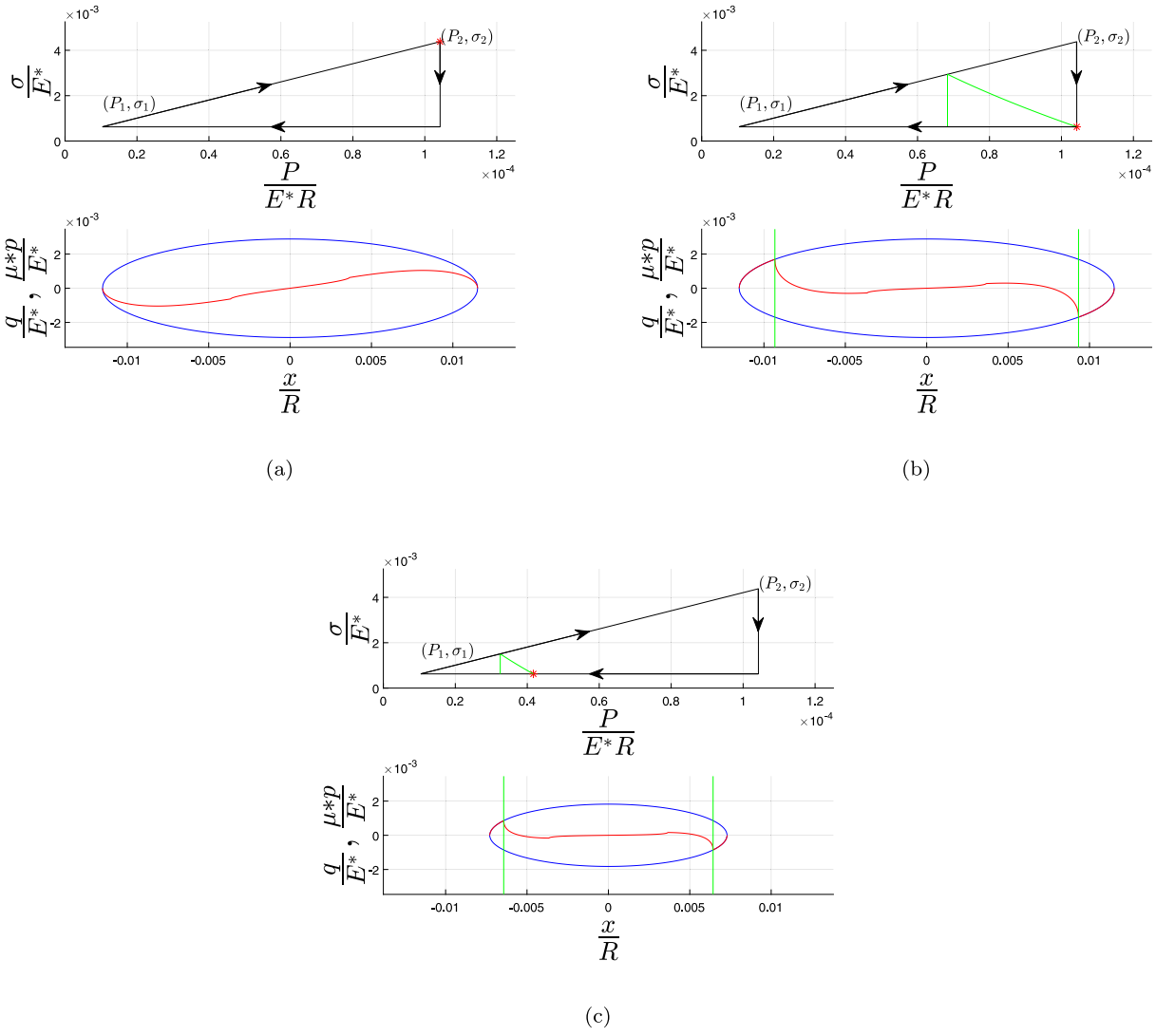

Fig. 6. The shear traction and stick zone constructions for a Hertzian contact following a right angled triangular loop in the clockwise direction. (a) The shear traction distribution at the end of the first stage of loading for the clockwise direction loop. The contact has been loaded proportionally from (P_1,σ_1) to (P_2,σ_2) locking in a distribution of shear traction, (b) The shear traction distribution for a Hertzian contact under a clockwise loading cycle at the end of the second step of loading. The applied bulk tension has been reduced from σ_2 to σ_1 at a constant normal load, creating a zone of slip, (c) The shear traction distribution at a point along the third step of the clockwise loading cycle. The normal load is being reduced from P_2 to P_1 at a fixed bulk tension, σ_1. During this stage of unloading a slip zone follows the edge of contact as it shrinks, with all particles in the zone $a_2 > x > a_1$ experiencing slip.

the second stage of loading that has not been erased. The size of the slip zone at a normal load P^* is found from the intersection of a construction curve with negative gradient with the construction from the end of step 2, Eq. (16) and the resulting shear traction is

$$q(x;P^*) = q_{FS}(x;P_{kL}) + q_{PS}(x;P_k;P_{kL}) - q_{PS}(x;P^*;P_k) \tag{21}$$

At the end of this step the reverse slip zone will be defined by load P_{kU}, which is larger than P_{kL}. The constructions for the stick zone are shown in Fig. 5(b), and consist of a line defined by (14) emanating from the current load point and a line defined by (15) emanating from (P_2,σ_2), with their intersection defining P_k.

The contact has now shaken down, and its behaviour is in a steady state. In the following step of the load cycle the contact is reloaded from (P_1,σ_1) to (P_2,σ_2), forward slip occurs again during this step as the gradient of loading is greater than the full stick condition. The size of the slip zone is found from the intersection of a construction curve with positive gradient emanating from the current load point (Eq. (15)) with the construction curve from the end of step 2 (Eq. (14) from point (P_1,σ_1)), as shown in Fig. 5(c). The shear traction is therefore given by

$$q(x;P^*) = q_{FS}(x;P_{kL}) + q_{PS}(x;P_{kU};P_{kL}) - q_{PS}(x;P_k;P_{kU}) + q_{PS}(x;P^*;P_k) \tag{22}$$

At the end of this step of the loading cycle P_k will be equal to P_{kU}. This can be seen graphically in Fig. 5(c): at the end of this load step the red and upper green construction lines will be coincident. The third term of the shear traction distribution will therefore be erased.

The final step to consider is the unloading of the contact in the steady state. Again reverse slip will occur, the construction being the same as in step 2, the intersection of a construction curve with negative gradient (Eq. (15)) with the construction line from the second step of loading, this is illustrated in Fig. 5(d). The resulting shear traction is therefore given by

$$q(x;P^*) = q_{FS}(x;P_{kL}) + q_{PS}(x;P_{kU};P_{kL}) + q_{PS}(x;P_k;P_{kU}) - q_{PS}(x;P^*;P_k) \tag{23}$$

At the end of this step of the load cycle P_k will be equal to P_{kU}, in Fig. 5(d) this can be seen graphically, the blue line will be coincident with the lower green line. The third term of the shear traction expres-

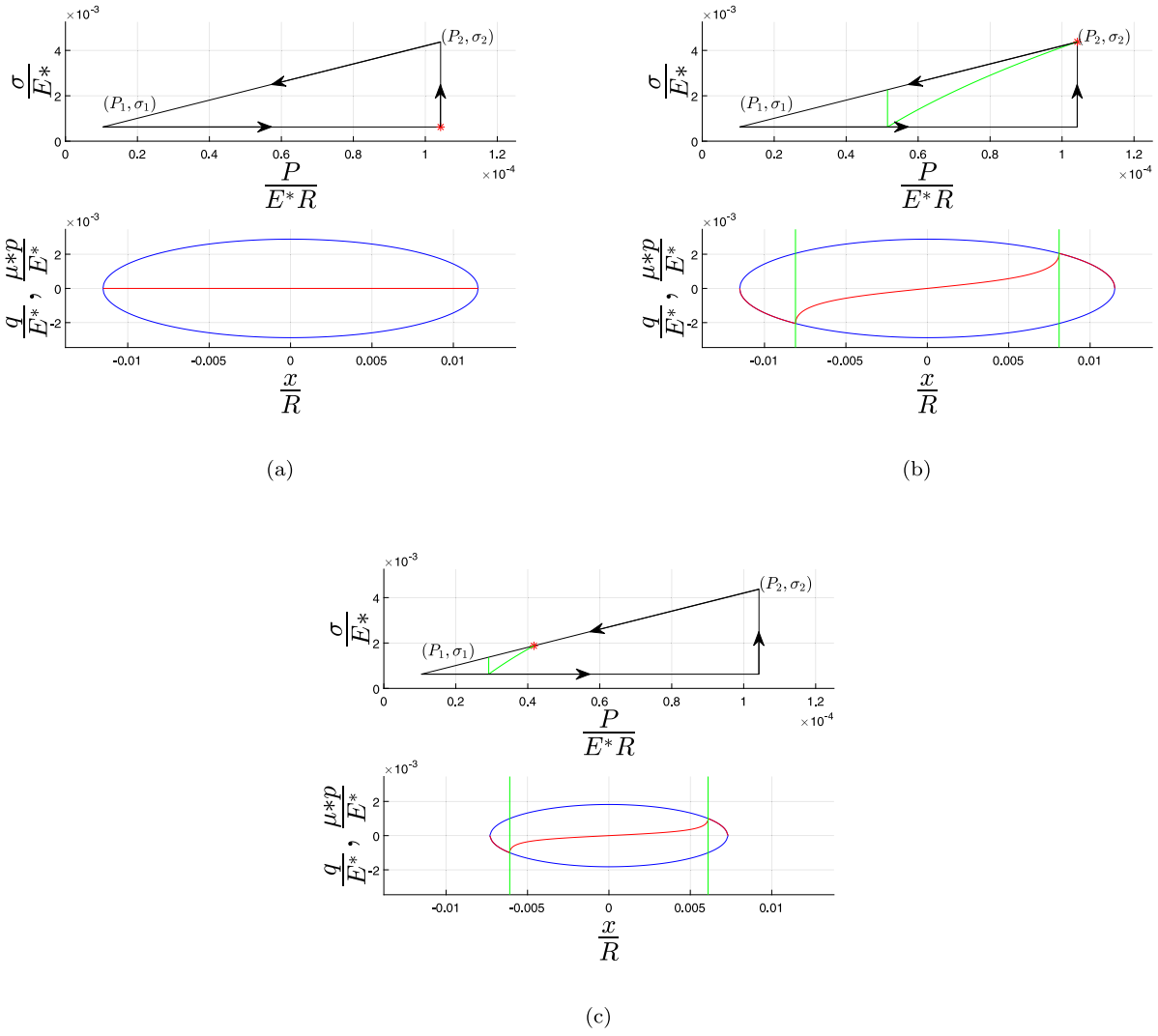

Fig. 7. The shear traction and stick zone constructions for a Hertzian contact following a right angled triangular loop in the anticlockwise direction (a) The shear traction distribution at the end of the first stage of loading. The contact has been loaded from P_1 to P_2 at constant bulk tension, so the contact interface is traction free, (b) The shear traction distribution at the end of the second stage of loading. A bulk tension has been applied at a fixed normal load, creating a slip zone, (c) The shear traction distribution at a point along the third stage of loading. The normal load and bulk tension are remove together in a proportional manner. as the contact is unloaded the slip zone size follows the edge of the contact, so that all points in the region $a_2 > x > a_1$ experience slip.

sion is therefore erased and the shear traction is the same as it was at the end of the third step of loading, showing that we have indeed reached the steady state.

By combining the principles discussed in Section 4 with those discussed above it is possible to create much more complex load paths involving multiple straight line stages of loading and unloading.

Fig. 4 shows a number of examples of load paths of this form, by unloading along the same path used for loading, closed load paths suitable for use in fretting fatigue tests can be created. If a contact is stuck during the loading section of the load cycle it will remain stuck when unloaded along the same path. For loading paths where slip occurs during loading, reverse slip will occur during unloading, with the method of finding the size of the reverse slip zone being as described in this section.

Load cycles with the form of two straight line segments have a number of desirable properties when used in fretting fatigue tests. By following different two step load paths between the same pair of points in load space we can create experiments where a contact is exposed to the same remote stress field, but where the existence of slip, the shear traction distributions and the slip displacements vary.

6. Triangular loading loops

One form of loading that has recently become of interest in our experimental work is those where the loading path and unloading path are different, so that the path travelled forms a loop. Ramesh et al. [5] considered a problem consisting of an elliptical loop in (a, σ) space, here we will discuss some solutions formed from straight line loading segments. These load paths have the useful property that slip only occurs in one direction, so via their use it is possible to investigate the effect of slip direction on fretting fatigue life.

6.1. Right-angled triangular loops

One way of forming a load path in the form of a loop is to combine a proportional and sequential load cycle. A contact travels between two points in load space, (P_1, σ_1) and (P_2, σ_2), alternately following proportional or sequential paths. This results in a load path having the form of a right angled triangle, as shown below in Fig. 6. The behaviour of the contact and the resulting size of the slip zones vary depending upon which direction of loading is followed. The values of the load points are chosen so that the straight line proportional loading from (P_1, σ_1) to (P_2, σ_2) is under conditions of full stick.

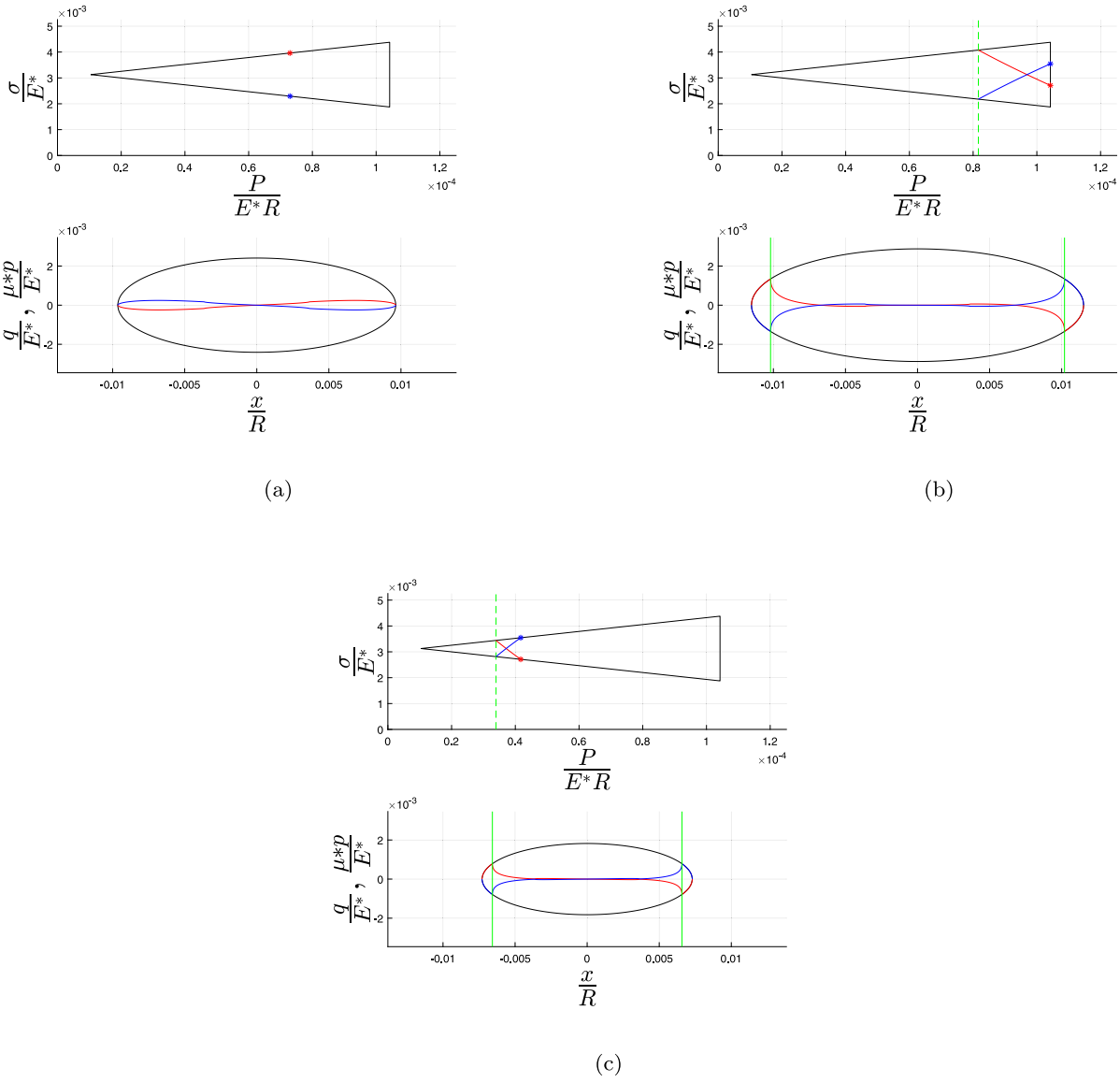

Fig. 8. The shear traction distributions and slip zone constructions for a contact under an isosceles triangle load path, showing the symmetry of the solution in the clockwise and anticlockwise directions. (a) The shear traction distribution at a point along the first step of loading, a proportional loading, with clockwise and anticlockwise solutions superimposed, (b) The shear traction distribution and slip zone constructions during the second step of an isosceles load path, during which the bulk tension is applied or removed at contant normal load, (c) The shear traction distribution and slip zone constructions during the final step of an isosceles load path, a proportional unloading.

6.1.1. Clockwise loading

Let us first consider a contact traversing the load path in a clockwise direction, when viewed as in Fig. 6, so that the load cycle consists of proportional loading followed by sequential unloading. In the following discussion we start from the point of minimum load (P_1, σ_1) and proceed around the cycle in a clockwise direction.

During the first step of loading the contact remains fully stuck and a distribution of shear traction is laid down as discussed in Section 2, the resulting shear traction is shown in Fig. 6(a). While no slip occurs this does not mean that there is no displacement between the bodies, due to the applied bulk tension points that were opposite each other at point (P_1, σ_1) will be displaced tangentially relative to the other body at (P_2, σ_2) as the bodies deform while out of contact.

During the second stage of this load cycle the contact is unloaded from σ_2 to σ_1 at constant normal load. This results in the creation of a slip zone, with the size of the remaining stick zone given by the intersection of a line defined by Eq. (14) and the original proportional loading path. The shear traction distribution and stick zone construction is illustrated in Fig. 6(b). It is worth noting here that the shear traction resulting from the unloading stage of the cycle are of the opposite sign to those that were locked in during the proportional loading step.

The final step of the load cycle consists of unloading the applied normal load at constant bulk tension σ_1. As the gradient of unloading during this step is less than the slip limit defined in Section 2.2 (in this case it is 0) slip will continue in the same direction as the second step of loading. The construction is the same as that used in the second step of the cycle, it can be seen that as the size of the contact reduces a slip zone of continuously reducing size will follow the edge of contact until the size of the contact again reaches a_1.

6.1.2. Anticlockwise loading

Let us now consider the behaviour of the contact when we reverse the direction of the loading cycle, so that the cycle consists of a sequential loading followed by a proportional unloading. The first stage of this cycle consists of applying normal load alone, so that the contact reaches its maximum extent but with a traction free interface, Fig. 7(a). In this case points which were opposite each other in the unloaded

contact will remain opposite each other in the contact at its full extent — there is no tangential displacement.

In the second stage of this load cycle the contact is loaded at a constant value of P from σ_1 to σ_2, which results in the formation of a slip zone. The construction defining the size of the slip zone is the intersection of Eq. (15) with a line of constant σ, $\sigma = \sigma_1$. This is equivalent to the solution for the constant normal load case. The shear traction and stick zone size construction is shown in Fig. 7(b).

In the final step of this load cycle the contact is unloaded along a proportional load path. As the gradient of unloading is less than the frictional slip limit at all points along this unloading slip will continue in the same direction as step 2. Fig. 7(c) shows the stick zone construction and resulting shear traction for a point along this step of the loading cycle.

6.1.3. Comparison and commentary

In comparing the clockwise and anticlockwise load paths a number of stark differences are evident. The first of these worth noting is that the clockwise loading cycle creates shear tractions in the contact interface that reverse direction during the loading cycle, while in the anticlockwise loop the shear traction is always in the same direction. All material must return to its original position by the end of the cycle, but in the latter case rather than occurring as reversing slip this occurs as tangential displacements while the two components are separated.

Another point worth noting is the drastic difference in the size of the stick zone. At the end of the constant normal load application or removal of bulk tension the stick zone is much smaller in the anticlockwise cycle than in the clockwise one; this can clearly be seen from the much reduced value of P_K in Fig. 7(b) when compared to 6(b). This difference occurs because in the anticlockwise load cycle the slip is extending into a region where there is a pre-existing shear traction distribution which opposes the growth of the slip zones, while in the clockwise case the slip is extending into a traction free interface.

6.2. Isosceles triangular loops

One potentially useful modification of the right angled triangular load path discussed previously involves constructing a load path that has the same behaviour in the clockwise and anticlockwise directions. One such load path that can be constructed entirely from straight line loading segments has the form of an isosceles triangle, as shown in Fig. 8. By following a load path of this form the shear tractions present are have the same distribution but opposite sign when the direction of loading is reversed.

The first step of this load cycle is a proportional loading under full stick. The shear traction solution during this step is the same as the solution given in Section 2. The shear traction distribution at a point along this step of the loading cycle is shown in Fig. 8(a), showing the symmetry of the shear traction distribution.

In the second step of this loading cycle the contact undergoes a change in the bulk tension load at a constant normal load, resulting in the formation of a slip zone. The size of the stick zone is given from the intersection of a curve defined by Eq. (14) or (15) with the initial proportional loading, depending upon the direction of travel. This is illustrated in Fig. 8(b), which shows the symmetrical constructions for both clockwise (red) and anticlockwise (blue) load paths. Again, it can be seen that, for equivalent points on the clockwise and anticlockwise loading cycles, the stick construction is identical, so therefore the slip zones are also the same size.

Finally the contact is unloaded along a proportional straight line path back to the starting load point. Once again the gradient of unloading is less than the condition for no full stick, so slip will continue in the same direction as the second step, with the size of the stick zone is found from the intersection of the curve construction, as shown in Fig. 8(c). As in the right angled load path a small slip zone follows the edge of contact as it is unloaded, such that the entire change in contact experiences slip at some point in the cycle.

7. Conclusion

In this paper we have presented an overview and compilation of methods for finding the slip behaviour and shear traction distribution for incomplete contacts under various paths in $P - \sigma$ space. These solutions are applied to a number of novel load paths which have desirable properties when used in fretting fatigue experiments. By using both sequential and proportional load paths it is possible to set up two tests with the same start and end points, but where in one load cycle the contact remains fully stuck and the other experiences partial slip; this allows the effect of slip to be largely decoupled from the remotely applied loads and the stress field within the body of the specimen. The triangular load paths presented experience slip in only one direction, so that by using combinations of clockwise and anticlockwise load cycles the effect of slip direction and the difference between unidirectional and reversing slip can be isolated and studied. Combined, load paths of these forms provide a useful toolbox for investigating the fundamental causes of fretting fatigue and investigating what effect slip has on the life of the contact.

Declaration of competing interest

The authors declare that they have no known competing financial interests or personal relationships that could have appeared to influence the work reported in this paper.

Data availability

Data will be made available on request

Acknowledgements

James Truelove acknowledges with thanks the award of an iCASE award ref 17000027 from Rolls-Royce plc which has enabled him to carry out this work.

David Hills and Luke Blades acknowledge Rolls-Royce plc, United Kingdom and the EPSRC, United Kingdom for their support under the Prosperity Partnership Grant “Cornerstone: Mechanical Engineering Science to Enable Aero Propulsion Futures”, Grant Ref: EP/R004951/1.

References

[1] Barber J, Davies M, Hills D. Frictional elastic contact with periodic loading. Int J Solids Struct 2011;48(13):2041–7.

[2] Hills D, Davies M, Barber J. An incremental formulation for half-plane contact problems subject to varying normal load, shear, and tension. J Strain Anal Eng Des 2011;46(6):436–43.

[3] Nowell D, Hills D. Mechanics of fretting fatigue tests. Int J Mech Sci 1987;29(5):355–65.

[4] Ciavarella M, Macina G. New results for the fretting-induced stress concentration on hertzian and flat rounded contacts. Int J Mech Sci 2003;45(3):449–67.

[5] Ramesh R, Barber J, Hills D. Plane incomplete contact problems subject to bulk stress with a varying normal load. Int J Mech Sci 2017;122(January):228–34.